HHS Public Access

Author manuscript

J Immunol. Author manuscript; available in PMC 2017 August 15.

Published in final edited form as:

J Immunol. 2016 August 15; 197(4): 1425–1434. doi:10.4049/jimmunol.1600264.

G2A signaling dampens colitic inflammation via production of IFNγ

S. Courtney Frasch[*,2], **Eóin N. McNamee**[†], **Douglas Kominsky**[†,3], **Paul Jedlicka**[‡], **Claudia Jakubzick**[*,§], **Karin Zemski Berry**[¶], **Matthias Mack**[‖], **Glenn T. Furuta**[#], **James J. Lee**[**], **Peter M. Henson**[*], **Sean P. Colgan**[†,††], and **Donna L. Bratton**[*,††]

[*]Department of Pediatrics, National Jewish Health, Denver, CO 80206, USA

[†]Mucosal Inflammation Program, Department of Anesthesiology, University of Colorado, Anschutz Medical Campus, Aurora, CO 80045, USA

[‡]Department of Pathology, University of Colorado, Anschutz Medical Campus, Aurora, CO 80045, USA

[§]Department of Immunology and Microbiology University of Colorado, Anschutz Medical Campus, Aurora, CO 80206, USA

[¶]Department of Pharmacology, University of Colorado Denver, Anschutz Medical Campus, Aurora, CO 80045, USA

[‖]Department of Internal Medicine, University of Regensburg, 93042 Regensburg, Germany

[#]Digestive Health Institute, Children's Hospital Colorado; Gastrointestinal Eosinophilic Diseases Program, Department of Pediatrics, University of Colorado School of Medicine, Aurora, CO 80045, USA

[**]Division of Pulmonary Medicine, Department of Biochemistry and Molecular Biology, Mayo Clinic in Arizona, Scottsdale, AZ, 85259, USA

Abstract

Pro-inflammatory consequences have been described for lysophosphatidylcholine, a lipid product of cellular injury, signaling via the g-protein coupled receptor G2A on myeloid and lymphoid inflammatory cells. This prompted the hypothesis that genetic deletion of G2A would limit intestinal inflammation in a mouse model of colitis induced by dextran sodium sulfate. Surprisingly, $G2A^{-/-}$ mice exhibited significantly worsened colitis compared to wild type mice as demonstrated by disease activity, colon shortening, histology, and elevated IL-6 and IL-5 in colon tissues. Investigation of inflammatory cells recruited to inflamed $G2A^{-/-}$ colons showed significantly more $TNF\alpha^{+}$ and $Ly6C^{hi}MHCII^{-}$ "pro-inflammatory" monocytes and eosinophils than in wild type colons. Both monocytes and eosinophils were pathogenic as their depletion abolished the excess inflammation in $G2A^{-/-}$ mice. $G2A^{-/-}$ mice also had less IFNγ in inflamed colon tissues than wild type mice. Fewer $CD4^{+}$ lymphocytes were recruited to inflamed $G2A^{-/-}$

[2]Corresponding author: S. Courtney Frasch, Ph.D. National Jewish Health, 1400 Jackson Street, A536, Denver, CO 80206, USA. Fax: 303-398-1380, Phone: 303-398-1227, fraschc@njhealth.org.

[††]These authors contributed equally to this work.

[3]Current address is Department of Microbiology and Immunology, Montana State University, Bozeman, MT 59717, USA

colons and fewer colonic lymphocytes produced IFNγ upon *ex vivo* stimulation. Administration of IFNγ to G2A$^{-/-}$ mice during dextran sodium sulfate exposure abolished the excess colitic inflammation, and reduced colonic IL-5 and eosinophil numbers to levels seen in WT mice. Further, IFNγ reduced the numbers of TNFα^{+} monocyte and enhanced their maturation from Ly6C^{hi}MHCII^{-} to Ly6C^{int}MHCII^{+}. Taken together, the data suggest that G2A signaling serves to dampen intestinal inflammation via the production of IFNγ, which in turn, enhances monocyte maturation to a less inflammatory program and ultimately reduces eosinophil-induced injury of colonic tissues.

Introduction

The inflammatory bowel diseases (IBD), including both ulcerative colitis (UC) and Crohn's disease, are debilitating mucosal disorders of unknown etiology (1). The most recent evidence suggests IBD results from an inappropriately directed inflammatory response to the intestinal microbiota in a genetically susceptible host. Epithelial cells are crucial in the maintenance of colonic tissue homeostasis, as IBD is characterized by a breakdown of the intestinal epithelial barrier leading to increased exposure of the mucosal immune system to antigenic luminal material. Since the epithelium functions as the critical interface between the intestinal lumen and the sub-epithelial mucosa, it is thereby anatomically positioned as a central coordinator of mucosal inflammatory response.

Studies to date indicate that cytokines and chemokines that are produced locally at sites of inflammation play an important role in onset and progression of IBD. IFNγ, present in IBD, has been shown to have a pro-inflammatory role in a number of autoimmune and inflammatory diseases (1, 2). The dextran sodium sulfate (DSS) model of murine colitis results from direct epithelial injury followed by recruitment of inflammatory cells and their inappropriate response to the microflora of the gut (3). The acute phase is characterized by the production of pro-inflammatory cytokines, including IFNγ, similar to that observed in human IBD (4–7).

The g-protein coupled receptor, Gpr132 (G2A) is expressed on most leukocytes, *e.g.* lymphocytes, monocytes, and granulocytes (www.immgen.org (8)). Signaling by G2A is poorly understood, and varies widely depending on its activator and the responding cell type and inflammatory context (8). One such stimulant is lysophosphatidylcholine (lysoPC), a lipid produced by injured epithelium *e.g.* in the airways (9, 10) and colon (11, 12). LysoPC signaling through G2A induces chemotaxis of monocytes, macrophages, and lymphocytes (13–15) and enhances the production of reactive oxygen species (ROS) by phagocytes (16, 17) and IFNγ from lymphocytes (18).

Given the observations noted above that G2A signaling heightens inflammatory cell recruitment and host defense responses, we hypothesized that deficiency of G2A, or antagonism of its signaling, would be beneficial in colitis. However, contrary to our hypothesis, genetic deficiency of G2A resulted in significantly worsened colitis in the knockout (G2A$^{-/-}$) mice compared to wild type animals (WT). These data demonstrate that while production of lysoPC was similar in both G2A$^{-/-}$ and WT mice during DSS exposure, deficient IFNγ production within colon tissues of the G2A$^{-/-}$ mice led to worsened injury

that was rectified by exogenous administration of IFNγ. These data support the unexpected conclusion that signaling via the g-protein coupled receptor G2A serves to counterbalance over-exuberant innate immune cell injury in DSS colitis via the enhanced production of IFNγ.

Methods

Reagents

Anti-CD45 BV510 or APC, anti-Ly6C APC-Cy7, anti-Ly6G PE, anti-MHCII BV421, anti-CD11b PerCPCy5.5, anti-CD11c PE-Cy7, anti-IFNγ PE, anti-TNFα APC, anti-CD3 PerCPCy5.5, anti-CD8 PE, anti-CD4 APC-Cy7, anti-NKp46 PE-Cy7, anti-B220 Alexa488 were from Biolegend (San Diego, CA). Anti-CD16/32 (Fc-block), anti-SiglecF PE and anti-F4/80 Alexa488 were from BD Biosciences (San Diego, CA). Blue fixable Live/Dead was from Invitrogen. Anti-CCR2 (clone MC-21) was provided by Dr. Matthias Mack. Anti-IL5 (clone TRFK5) was provided by Dr. James Lee (Mayo Clinic, Scottsdale, AZ). Recombinant mouse IFNγ was from R&D Systems. Collagenase D was from Roche Diagnostics (Indianapolis, IN) and Collagenase VIII was from Sigma-Aldrich (St. Louis, MO). 1-oleoyl-2-hydroxy-*sn*-glycerol-3-phosphocholine (LPC) was from Avanti Polar Lipids, Inc. (Alabaster, AL).

Mice

Male and female C57BL/6 (WT) mice were purchased from The Jackson Laboratory (Bar Harbor, ME) and were generated from a breeding colony at National Jewish Health (Denver, Colorado). $G2A^{-/-}$ breeder pairs on a C57BL/6 background were a generous gift from Dr. Catherine Hedrick and were bred in-house. All animals received care in accordance with the guidelines of the Institutional Animal Care and Use Committee and were maintained on food and water *ad libitum*. Mice between the ages of 8 and 12 weeks were used and were age and gender-matched for all experiments. WT and $G2A^{-/-}$ mice were co-housed for 7–10 days prior to induction of colitis. Preliminary experiments demonstrated that the results following 7 days co-housing were identical to those following 14 days of co-housing.

Induction of colitis and treatments

Experimental colitis was induced in mice by adding 3% (w/v) DSS (m.w. 36,000–50,000; MP Biomedicals, Santa Ana, CA) to drinking water for various numbers of days (2–6d, as indicated). Fresh DSS solutions were replaced at 3d. The animals were monitored daily for disease activity using the parameter of weight loss, stool consistency and fecal blood. Disease activity index (DAI) was calculated, as described by Cooper *et al.* (19), as the sum of scores of stool consistency (0=normal; 1= near normal; 2=loose stool; 3= very loose stool; 4= diarrhea) and establishment of ulceration of the colon as detected by blood in the feces (0=negative; 1=near negative; 2–3=positive; 4=gross bleeding) for a maximum score of 8. On the final day mice were humanely euthanized and colons were harvested. Colon length was measured as an indicator of disease severity. For depletion of monocytes, 20μg anti-CCR2 (clone MC-21) or isotype control was injected intraperitoneally (*i.p.)* on 5 consecutive days starting at day 1 after administration of DSS. For depletion of eosinophils, 200μg anti-IL-5 (clone TRFK5) or isotype control was injected *i.p.* on 5 consecutive days

starting on day 1 after administration of DSS. For IFNγ restoration experiments, mice received 5μg recombinant mouse IFNγ (R&D Systems) *i.p.* on days 3 and 5 after administration of DSS.

Histology

Sections from the distal colon of each mouse were fixed in 10% formalin before staining with H&E. All histological quantitation was performed blinded by a trained pathologist (P.J.). Colitis severity was determined by three independent parameters as described previously (20). Severity of inflammation (0–3: none, slight, moderate, severe), extent of injury (0–3: none, mucosal, mucosal and submucosal, transmural), and crypt damage (0–4; none, basal one-third damaged, basal two-thirds damaged, only surface epithelium intact, entire crypt and epithelium lost). The score of each parameter was multiplied by a factor reflecting the percentage of tissue involvement (X1: 0–25%, X2: 26–50%, X3: 51–75%, X4: 76–100%) and all numbers were summed for a total histologic index.

Isolation of colonic lamina propria leukocytes and splenocytes

Colons were opened longitudinally and flushed with PBS to remove contents and cut into 1cm pieces. Epithelial cells were depleted by incubation in 15mL HBSS (Mediatech, Manassas, VA) supplemented with 15mM HEPES (pH7.2), 2 mM EDTA and 2% heat-inactivated FBS (Atlanta Biologicals, Lawrenceville, GA), 100μg/ml streptomycin and 100 units/ml penicillin at 37°C for 40 min with constant shaking. The epithelial cell depleted colon tissue was washed in PBS to remove the EDTA, minced and digested in 10mL RPMI 1640 supplemented with 15mM HEPES (pH7.2), 5% heat-inactivated FBS (Atlanta Biologicals, Lawrenceville, GA), 2mM L-glutamine, 100μg/ml streptomycin, 100 units/ml penicillin, 1.2mg/mL collagenase D and 0.85 mg/ml collagenase VIII for 30 min at 37°C with constant shaking. Digested colon cells were passed through a 100μm filter to remove undigested tissue and the cells were centrifuged at 200 × *g* for 10 minutes. Total cells from colon digests were determined by coulter counts and cells were either cultured *ex vivo* or stained for analysis by flow cytometry (see below).

After the spleen was harvested from untreated mice, a single cell suspension was obtained by manually disrupting spleens through a 70-μm cell strainer (BD Falcon, Bedford, MA) with HBSS. Following lysis of red blood cells, the splenocytes were refiltered with a 40-μm cell strainer and resuspended at 2.5×10^6 cells/ml in RPMI 1640 supplemented with 15mM HEPES (pH7.2), 0.1% BSA, 2mM L-glutamine, 100μg streptomycin and 100 units/ml penicillin and stimulated as described below.

Flow cytometry

Isolated lamina propria cells were incubated with Fc block, stained with antibodies and flow cytometry was performed on a BD LSRII or BD LSRFortessa. Data were analyzed on FlowJo X v.10.0.7 (Tree Star). See Supplemental Figure 1 for gating strategy. Briefly, immune cell subsets were identified among live $CD45^+$ cells after doublet exclusion. For determination of colonic tissue or colonic vascular localization of lamina propria leukocytes, 5μl of anti-CD45 APC in 200μl PBS was injected intravenously (*i.v.*) 5 minutes before euthanasia. This method allows for the differential identification of cells that are

extravascular (at least excluded from antibody labeling) and likely located within the colonic tissue versus cells that are within the colonic vascular lumen. Total cell subsets were determined by multiplying the percentage of the cell subset, as determined by flow cytometry, by the total cell counts.

Culture and stimulation of colon tissue digests and spleen cells

For culture *ex vivo*, 1×10^6 digested colon cells in 200μl RPMI 1640 supplemented with 10% heat-inactivated FBS (Atlanta Biologicals, Lawrenceville, GA), 15mM HEPES (pH 7.4), 2mM L-glutamine, 100μg/ml streptomycin and 100 units/ml penicillin were left unstimulated or stimulated with 1× cell stimulation cocktail (PMA plus Ionomycin; eBioscience, San Diego, CA) in the presence or absence of 1× protein transport inhibitor (brefeldin A and monensin; eBioscience) for 4 hours at 37°C. Cell free supernatants were analyzed for IFNγ or TNFα by ELISA (ELISA Tech, Aurora, CO). Cells treated with protein transport inhibitor were stained for surface markers, fixed and permeabilized with the Fox P3 permeabilization kit (eBioscience) according to the manufacturers instructions for intracellular staining of IFNγ and TNFα. For *ex vivo* stimulation of naïve spleen cells, 0.5×10^6 spleen cells in 200 μl RPMI supplemented with 0.1% BSA, 15mM HEPES (pH 7.4), 2mM L-glutamine, 100μg/ml streptomycin and 100 units/ml penicillin were left unstimulated or stimulated with 0.5× stimulation cocktail in the absence or presence of 10μM LPC. A 10× stock of LPC was made by drying the LPC under a flow of nitrogen in a glass tube and resuspending in RPMI supplemented with 0.1% BSA. LPC was dissolved by sonication in a water bath sonicator. LPC was added simultaneously with the stimulation cocktail. Cell free supernatants were analyzed for IFNγ by ELISA (ELISA Tech, Aurora, CO).

Cytokine determinations

Pro-inflammatory cytokines were measured by using the MesoScale Discovery Platform (Pro-inflammatory Panel 1, MSD, Rockford, MD) in serum obtained following cardiac puncture or homogenates from sections of distal colon according to the manufacturers instructions.

Quantitative PCR

Sections from distal colon were snap frozen and stored at −80°C. Total RNA was isolated using the Qiagen mini RNA isolation kit (Qiagen, Inc) according to the manufacturers instructions and reverse transcribed using iScript cDNA Synthesis Kit (Bio-Rad, Hercules, CA). Real time quantitative PCR was performed and data were normalized to *GusB* and calculated as relative quantity ($2^{-\Delta\Delta Ct}$, where Ct is cycle threshold for each sample). The indicated forward and reverse primer pairs were purchased from Bio-Rad.

Lysophospholipid measurement

Colon tissues were collected, weighed and homogenized in MeOH/water (50:50). Lysophosphatidylcholine (lysoPC) internal standard (17:1/OH-PC) was added and total lipids were extracted by the method of Bligh and Dyer (21). The organic layer was collected and brought to dryness. Phospholipid classes were separated by application to an

aminopropyl SepPak (NH2-DSC) column and lysoPC was eluted with MeOH. LysoPC was measured in positive ion mode by precursors of m/z 184 by LC-MS/MS as previously described (22). For lysophosphatidylserine (lysoPS) measurements, colon tissues were collected, weighed, minced and extracted in MeOH. LysoPS internal standard (17:1/OH-PS) was added and insoluble material was centrifuged at 10,000 × g for 10 minutes. The MeOH supernatant was applied to an aminopropyl SepPac (NH2-DSC) column to separate lipid classes and lysoPS was eluted in ammonium hydroxide:MeOH 10:90 (v/v). LysoPS species were monitored by multiple reaction monitoring (MRM) by LC-MS/MS in negative ion mode as described previously (23).

Statistical analysis

Data are presented as the means ± SEM. Data represent 3–5 mice per group and at least two independent experiments unless otherwise stated. Unpaired *t* test, one-way or two-way ANOVA test were used to determine differences between groups, as indicated, where $p < 0.05$ was considered significant (GraphPad Prism, La Jolla, CA).

Results

G2A deficiency does not alter intestinal homeostasis but results in worsened DSS-induced colitis

Initial studies confirmed the lack of intrinsic intestinal inflammation in naïve mice globally deficient for G2A. Histologic examination of colonic tissues showed no epithelial disruption or obvious inflammation in either $G2A^{-/-}$ or WT mice at baseline (Supp. Fig. 1A). Colon lengths and lysoPC levels were no different between the two genotypes in the naïve state (Supp. Fig.1B and 1C). $CD45^{+}$ cells in digests of colonic tissues were examined by flow cytometry (see gating strategy in Supp. Fig. 1D). There were no baseline differences between the genotypes with regard to total numbers of macrophages, monocytes, eosinophils, neutrophils or lymphocytes (data not shown). As expected, G2A was expressed in the $CD45^{+}$ cells from WT colons but not from the $G2A^{-/-}$ colons, whereas isolated colonic epithelial cells were negative for G2A expression in both genotypes (data not shown). Total colon tissue was also analyzed by qPCR for pro-inflammatory cytokines, TNFα, IL-6, IL-1β, IFNγ, IL-12p70, IL-4, IL-13 and IL-5. Expression levels were very low or undetectable and no significant differences were noted between the genotypes (data not shown).

In a well-described intestinal inflammation model (3, 4), DSS (3%) was added to drinking water of both $G2A^{-/-}$ and WT mice and continued for 6 days. Disease activity was calculated using the parameters of stool consistency and fecal blood, which were determined daily for each mouse as described in experimental procedures, with a maximum of 8 points (19). By day 3, disease activity was evident in some mice of both genotypes and became more severe with increasing duration of DSS exposure (Fig. 1A). Over the time course of DSS exposure, $G2A^{-/-}$ mice had significantly greater disease activity scores than WT mice, and by day 6, had overt diarrhea and bleeding into the stool. By day 6, most $G2A^{-/-}$ mice had reached criteria to be euthanized. $G2A^{-/-}$ mice tended to lose more weight over the course of DSS exposure than WT mice. On sacrifice at day 6, colon length was measured

and found to be significantly shorter in G2A$^{-/-}$ mice than WT animals (Fig. 1B). Histologic examination of colonic tissues at day 6 showed marked inflammatory infiltrates in both genotypes and almost complete loss of crypt architecture in the distal colons of the G2A$^{-/-}$ mice (Fig. 1C). Accordingly, blinded histologic scoring of colonic tissues was significantly worse for G2A$^{-/-}$ mice than for WT mice.

Recruited inflammatory cells (CD45^{+}) were analyzed by flow cytometry (Supp. Fig. 1E gating strategy) following digestion of the total colonic tissue. In DSS-induced colitis, monocytes are a prominent recruited inflammatory cell and are thought to be largely responsible for orchestrating responses to commensal microbes that result in further colonic injury (24–27). We found monocyte numbers to be increased in both genotypes over time of DSS administration, but were significantly more numerous in the G2A$^{-/-}$ mice by day 6 (Fig. 2A). Since signaling via G2A has been shown to mediate chemotaxis of inflammatory cells including monocytes (8, 13), it was important to determine whether the monocytes within the colons were similarly distributed in the tissues *vs.* vasculature in the two genotypes. To this end, mice were injected intravenously (*i.v.*) with anti-CD45 just prior to sacrifice to separately tag cells in the colonic intravascular compartment and thereby providing a snapshot of cells present in this compartment. As shown in Figure 2A, intravascular monocytes (those labeling with anti-CD45) peaked at day 2 in both genotypes and appeared to be equivalent. For the most part, monocytes were extravascular (or sequestered from the antibody) in the inflamed colons of both genotypes demonstrating no obvious deficiency in recruitment of monocytes or distribution in colonic tissues in G2A$^{-/-}$ mice during DSS colitis. Eosinophils in colonic tissues during DSS colitis mirrored monocytes (Fig. 2B). Their numbers rose over the first 4 days of colitis similarly in both genotypes with few appearing to be intravascular by anti-CD45 labeling. However, significantly more eosinophils were present in the colons of G2A$^{-/-}$ mice by day 6. Recruited neutrophils were much fewer than monocytes and eosinophils, and no differences between the genotypes were evident (Fig. 2C). Unlike the other myeloid cell types, intravascular neutrophils constituted a substantial proportion of total neutrophils, approximately 25–30% on days 2–4 of DSS exposure, in both genotypes.

Though DSS-induced colitis develops independently of lymphocytes in Rag$^{-/-}$ mice (28), we did assess the lymphocyte populations in the inflamed colons. A population of CD4 cells were recruited to the colons of WT mice, but were strikingly deficient in the colons of G2A$^{-/-}$ mice throughout DSS exposure (Fig. 2D). CD8 cells were present in colons of both genotypes and no differences in numbers were detected (Fig. 2E). NK cells (Fig. 2F) and B cells (not shown) were also recruited to inflamed colons in similar numbers for both genotypes.

Colon tissues were assessed for several pro-inflammatory cytokines and mediators reportedly produced during the acute phase DSS-induced colitis (4–7). Inflamed colon tissues harvested on day 6 from G2A$^{-/-}$ mice demonstrated significantly higher amounts of IL-6 and IL-5 in comparison to WT (Fig. 3A). In contrast, IFNγ levels in colon tissue were much lower in G2A$^{-/-}$ mice (Fig. 3B). No differences between the genotypes were seen for colon tissues levels of TNFα, IL-12p70, IL-1β, CXCL1 or IL-10 (data not shown). Message for CCL5, CCL11, CCL24, IL-13 and IL-4 was determined by qPCR with no differences

detected between the genotypes (data not shown). LysoPC, associated with injury of epithelium (11, 12), was also measured in colonic tissues from both genotypes over time. Importantly, LysoPC levels were elevated over baseline and appeared to peak at day 4 of DSS exposure but were no different between the genotypes (Fig. 3C).

In summary, the G2A$^{-/-}$ mice, relative to WT mice, showed significantly worsened disease on all measures, and showed increased numbers of monocytes and eosinophils and fewer CD4 lymphocytes recruited to injured colons than WT mice. Differences in cytokines present in colon tissues appeared to be elevated IL-6 and IL-5, and diminished IFNγ in the G2A$^{-/-}$ mice relative to WT.

Worsened colitis in G2A deficient mice is driven by pro-inflammatory monocytes in an eosinophil-dependent manner

Earlier studies from several groups have shown that monocyte populations infiltrating the inflamed colon exhibit marked heterogeneity, with transition over time from a so-called "pro-inflammatory" phenotype to an "anti-inflammatory" phenotype (26, 27). Pro-inflammatory Ly6C^{hi}MHCII^{-} monocytes are initially recruited from the blood to the tissues and have been shown to make TNFα in DSS colitis, and over time, they begin to lose Ly6C expression and gain MHCII expression. These Ly6C^{int}MHCII^{+} monocytes acquire "anti-inflammatory" features as they have been shown to produce IL-10 (26, 27). In the G2A$^{-/-}$ mice, the number of pro-inflammatory monocytes (Ly6C^{hi}MHCII^{-}) was significantly higher by day 6 of DSS-induced colitis relative to WT (Fig. 4A). The number of monocytes staining for intracellular TNFα were also significantly more numerous in the G2A$^{-/-}$ mice (Fig. 4B). On the other hand, numbers of Ly6C^{int}MHCII^{+} monocytes were no different between the genotypes. We were unable to identify IL-10 staining in monocytes of either genotype, attesting to the difficulty of intracellular staining for this cytokine, and as noted above, no differences between genotypes were observed in levels of IL-10 measured in colonic tissue.

Pro-inflammatory monocytes are thought to contribute to host/biome responses and injury in DSS-induced colitis (24, 25). For example, both the CCR2$^{-/-}$ mice and mice in which monocytes have been depleted show improvement in various endpoints in DSS colitis (27, 29). As such, the potential role of pro-inflammatory monocytes in driving the excess inflammation seen in the G2A$^{-/-}$ mice was assessed using a monocyte-depleting antibody. As shown in Fig. 5A, prior treatment with the anti-CCR2 (MC-21) antibody efficiently depleted monocytes from both genotypes regardless of phenotype. With monocyte depletion, the exacerbated disease activity and colon shortening in the G2A$^{-/-}$ mice was reduced to that seen in WT animals (Figs. 5B and 5C). Monocyte depletion in WT mice was associated with a trend toward lessened disease activity consistent with the findings by others (27, 30).

Notably, monocyte depletion abolished excess eosinophil numbers in the G2A$^{-/-}$ mice (Fig. 5D) indicating that monocytes can play a role in the accumulation of eosinophils as reported previously (29). Eosinophil accumulation in colonic tissue of DSS-treated WT mice was unchanged with monocyte depletion. No changes were seen in neutrophil or lymphocyte numbers in either genotype with monocyte depletion.

Using an antibody directed to IL-5 (clone TRFK5), excess eosinophil numbers were depleted in the G2A$^{-/-}$ mice (Fig. 6A), and their exacerbated colon shortening and disease activity were significantly reduced to that of WT mice (Fig.6B and 6C). Of note, eosinophils in WT mice were also reduced following anti-IL-5 antibody administration. However, in WT mice colon shortening was worsened and their disease activity was exacerbated, consistent with our previously published data (31). Thus, subpopulations of eosinophils clearly play differing roles in DSS-induced colitis depending on genotype: mediating the worsened colitis in G2A$^{-/-}$ mice, whereas ameliorating colitis in WT (see Discussion).

The role of IFNγ production in G2A$^{-/-}$ disease activity

IFNγ production in colitis is thought to come from several lymphocyte populations (32, 33). Given the lower levels measured in inflamed colonic tissues of the G2A$^{-/-}$ mice (Fig. 3), possibly related to the reduced numbers of CD4 lymphocytes recruited to the colons of these mice (Fig. 2), we further investigated the role of IFNγ. First, a time course of *Ifng* gene expression in whole colon tissue was assessed. *Ifng* mRNA in colonic tissues increased in WT mice by day 4 and was significantly elevated over baseline by day 6 (Fig. 7A). This increase was not evident in G2A$^{-/-}$ mice. The differences in the levels of IFNγ in inflamed colons between the two genotypes (Fig. 3) were also evident in sera (Fig. 7B).

Next, we assessed stimulated production of IFNγ from colonic digest cells. Cells (10^6) from DSS day 6 colon digests were cultured in media and stimulated with PMA and ionomycin for 4 hours and IFNγ assessed in the supernatants by ELISA. As shown, IFNγ was profoundly deficient in culture supernatants from G2A$^{-/-}$ mice in comparison to WT mice (Fig. 7C), whereas stimulated TNFα levels were not different between the genotypes. By contrast, PMA/ionomycin stimulated spleen cells from naïve G2A$^{-/-}$ and WT mice produced similar amounts of IFNγ (Fig. 7D) showing that the ability to produce IFNγ was not generally deficient in the G2A$^{-/-}$ animals. However, as hypothesized, only WT and not G2A$^{-/-}$ splenocytes made additional IFNγ in response to lysoPC treatment. To better define potential sources of IFNγ in the inflamed colons, colon digest cells were then stimulated as above in the presence of brefeldin A, stained for CD4 and intracellular IFNγ and analyzed by flow cytometry. Under these conditions, intracellular IFNγ was evident in a proportion of stimulated CD4$^+$ and CD4$^-$ lymphocytes (Fig. 7E). When expressed as a percentage of total lymphocytes for each genotype, fewer were positive for IFNγ in the G2A$^{-/-}$ animals than in WT (Fig. 7E). Thus, it appears likely that WT lymphocytes, most notably CD4$^+$ T cells, but also CD4$^-$ lymphocytes are recruited to injured colons, and are primed/stimulated in a G2A dependent manner for enhanced IFNγ production. In the absence of G2A signaling, fewer numbers of CD4$^+$ lymphocytes are recruited during colitis, and these lymphocytes, as well as recruited CD4$^-$ lymphocytes, are deficient in their production of IFNγ.

Ly6C^{int}MHCII$^+$ monocytes, in some settings, have been shown to bear an IFNγ response signature (34, 35). We hypothesized that deficient IFNγ in the colon of the G2A$^{-/-}$ mice might contribute to a blockade or delay in the transition of Ly6C^{hi}MHCII$^-$ pro-inflammatory monocytes to Ly6C^{int}MHCII$^+$ anti-inflammatory monocytes. To address this, G2A$^{-/-}$ mice were treated with IFNγ (5μg) on day 3 and day 5 of DSS exposure with harvest of the animals at day 6. Following IFNγ treatment, the total numbers of monocytes in the colons of

G2A$^{-/-}$ were unchanged and remained elevated compared to WT colons (Fig. 8A). However, following IFNγ treatment, the proportion of monocytes that were Ly6C^{hi}MHCII^{-} was significantly lower, and the Ly6C^{int}MHCII^{+} significantly greater in G2A$^{-/-}$ mice (Fig. 8A and Suppl. Fig. 2A). In support of the hypothesis that transition to Ly6C^{int}MHCII^{+} is associated with a less inflammatory program, the number of monocytes staining positive for intracellular TNFα was also reduced. Colon tissue IL-6 appeared to be reduced following IFNγ treatment of G2A$^{-/-}$ mice though the difference did not reach significance (Fig. 8B). Colon tissue IL-10 was no different (data not shown). IL-5 in colon tissues was significantly reduced following IFNγ treatment, and accordingly, eosinophil numbers were reduced to that seen in WT colon tissues (Fig. 8C).

Importantly, the exacerbated colitis in the G2A$^{-/-}$ mice was significantly ameliorated with IFNγ treatment (Fig. 8D). Disease activity, colon lengths and histology were all improved in G2A$^{-/-}$ mice with measures of each being similar to those seen in the WT mice, as well as substantially mimicking the effects of monocyte and eosinophil depletion (Figs. 5–6). Identical treatment of WT mice with IFNγ resulted in minimal reductions in disease activity, colon shortening, and cellular infiltration suggesting optimal effects from endogenously produced IFNγ (Suppl. Fig. 2B–D).

Discussion

Production of lysoPC accompanies epithelial cell injury in the airway (9, 10) and the intestine (11, 12), and results in a variety of pro-inflammatory actions mediated through the g-protein coupled receptor G2A present on recruited inflammatory cells (8). While our investigation of colitis in G2A$^{-/-}$ mice began with the hypothesis that loss of this receptor would be therapeutic, this hypothesis is refuted with unequivocal evidence that the g-protein coupled receptor serves to dampen inflammation in this model. Key elements were identified in this investigation: excess inflammation and disease activity in the G2A$^{-/-}$ mice were attributable to activities of pro-inflammatory subpopulations of monocytes and eosinophils, and surprisingly, injury from these effector cells was ultimately the result of diminished production of IFNγ.

IFNγ is elevated in colonic tissues in human inflammatory bowel disease as well as in animal colitis models (4–7). IFNγ is generally thought of as a quintessential pro-inflammatory cytokine required in many instances for innate and Th1 adaptive immunity, though its effects are protean. Genetic ablation of IFNγ or its neutralization has been shown by some (32, 36) but not other investigators (37) to ameliorate disease severity in the DSS model. These mixed findings and our data, here, may help to explain the lack of therapeutic success of blocking the action of IFNγ in human IBD (38).

The sources of IFNγ in DSS colitis are thought to be a various lymphocyte populations including both CD4 and CD8 cells after exposure to inflamed colonic epithelial cells (32). We have shown deficient recruitment of CD4 lymphocytes to inflamed colons in the G2A$^{-/-}$ mice and that recruited lymphocyte populations, both CD4^{+} and CD4^{-}, seem to produce less IFNγ in response to stimulation than lymphocytes of WT mice (Fig. 7). The most likely explanation is that the G2A$^{-/-}$ lymphocytes cannot be primed/activated for enhanced

production of IFNγ by lysoPC (18). In this regard, we note that the G2A receptor can also respond to other signals aside from lysoPC, *e.g.* lysoPS (39). We measured lysoPS and found it present at very low levels in both genotypes for most of the course of colitis (data not shown). Though we cannot rule out a contribution in WT mice from lysoPS/G2A anti-inflammatory modulation of monocyte programming (23), to our knowledge only lysoPC/G2A signaling has been associated with IFNγ production by lymphocytes (16, 18). Of note, in recent studies of DSS colitis and UC in humans it was shown that lysoPC ultimately declines with disease chronicity (12, 40), and given our findings, we hypothesize this may result in deficient G2A signaling and the resulting inflammatory events demonstrated here.

Despite the defined effect of G2A signaling on dampening the degree of colonic inflammation and disease in this model, a key future question is the specific cell target(s) for the G2A effect and the proposed effect of lysoPC stimulation. However, even in the absence of isolating G2A deficiency on one cell type or another, the approach taken here allowed us to elucidate specific roles and a hierarchy for the key effector cells/mediators. First, depletion of either eosinophils or monocytes using depleting antibodies, or the institution of IFNγ treatment, all resulted in nearly identical amelioration of the enhanced disease activity, histological changes and colon shortening in the $G2A^{-/-}$ mice (comparing Figs. 5, 6, and 8). Thus, a common pathway is suggested. Further support for this comes from the observation that both monocyte depletion and IFNγ treatment resulted in elimination of excess eosinophil numbers in the G2A deficient mice, whereas eosinophil depletion in these mice had no obvious effect on these other key elements. This allows us to position eosinophils as a candidate final effector cell responsible for excess colonic injury in the $G2A^{-/-}$ mice. An important observation is that whereas depletion of excess eosinophils in the $G2A^{-/-}$ mice was ameliorative of heightened inflammation and disease activity, depletion of eosinophils in WT animals exacerbated injury. This latter finding has been recently published and is attributed to deficient eosinophil 15-lipoxygenase production of protectin D1 (31). Further, intestinal eosinophils are present in the colon in homeostasis in both genotypes and not fully amenable to this depletion strategy. These data highlight the observations that eosinophils can play many immunomodulating roles differing in intestinal homeostasis and disease states (41, 42). Clearly their activation status, numbers and location are likely of great importance to such heterogeneity and the different roles that they play, and the potential role of G2A on eosinophils, themselves, are all key areas for further investigation.

Perhaps the most surprising finding in this investigation of colitis in the $G2A^{-/-}$ mice was the prominent role of IFNγ in the anti-inflammatory programming of recruited monocytes. Several groups have shown that monocytes recruited to the inflamed colon in the DSS model exhibit marked heterogeneity (26, 27). They are known to progress from $Ly6C^{hi}$ $MHCII^{-}$ TNFα-producing monocytes through loss of Ly6C and gain of MHCII in association with IL-10 production (26, 27). We have shown that treatment with IFNγ, while not affecting overall numbers of monocytes in $G2A^{-/-}$ mice, appeared to enhance the acquisition of MHCII on monocytes in the $G2A^{-/-}$ mice (Fig. 8A and Suppl. Fig. 2A), an effect consistent with actions of IFNγ in other contexts (33, 43). We were unable to replicate enhanced intracellular staining of IL-10 in the resulting $Ly6C^{int}MHCII^{+}$ monocytes in either WT or $G2A^{-/-}$ mice (data not shown), and levels of IL-10, known to be produced by other sources

in colitis (44–46), were not different between G2A$^{-/-}$ and WT colitic mice. Importantly, the enhanced transition of monocytes to Ly6C^{int}MHCII^{+} driven by IFNγ was accompanied by diminished numbers of TNFα^{+} monocytes (Fig. 8A). TNFα clearly plays an important role in the DSS model (47, 48) and human IBD where it is a proven therapeutic target (49–51). This anti-inflammatory activity of IFNγ on monocytes adds to accumulating evidence that IFNγ may display inflammation mitigating properties in mucosal inflammation models (52). IFNγ has, for example, been shown to mediate anti-inflammatory properties through induction of indoleamine 2,3-dioxygenase 1 (53), regulation of the methylation response (54) and induction of epithelial IL-10 receptors (20) supportive of healing responses by the epithelium. We also note that anti-inflammatory activities of IFNγ on monocytes have also recently been described in the context of gastrointestinal infection (43).

In summary, the g-protein coupled receptor G2A appears to be important in limiting disease severity in this model of acute colitis driven by insult to the epithelium and propagated by innate host response to microflora. G2A signaling does so through a complex interaction of IFNγ production, monocyte programming and eosinophil-induced injury. Investigation of its roles in chronic intestinal inflammation, other models of IBD, and in other models of epithelial insult *e.g.* airways, is likely to provide new mechanistic insights and possible therapeutic targets following mucosal injury.

Supplementary Material

Refer to Web version on PubMed Central for supplementary material.

Acknowledgments

The authors would like to thank Ruby Fernandez-Boyanapalli, Ph.D. and Joanne Masterson, Ph.D. for helpful discussions and Elizabeth Redente, Ph.D. and Erica Alexeev, Ph.D. for technical assistance.

This work was supported by HL34303 (DLB), AI110408 (DLB), HL114381 (PMH, CJ and DLB), DK104713 (SPC), DK099452 (DK), NIH K24 DK100303 (GTF).

Abbreviations used in this article

DSS	dextran sodium sulfate
lysoPC	lysophosphatidylcholine
IBD	inflammatory bowel disease
UC	ulcerative colitis
DAI	disease activity index
lysoPS	lysophosphatidylserine
qPCR	quantitative PCR
WT	wild-type.

References

1. Xavier RJ, Podolsky DK. Unravelling the pathogenesis of inflammatory bowel disease. Nature. 2007; 448:427–434. [PubMed: 17653185]
2. Peters CP, Mjosberg JM, Bernink JH, Spits H. Innate lymphoid cells in inflammatory bowel diseases. Immunology letters. 2015
3. Chassaing B, Aitken JD, Malleshappa M, Vijay-Kumar M. Dextran sulfate sodium (DSS)-induced colitis in mice. Current protocols in immunology / edited by John E. Coligan … [et al.]. 2014; 104(Unit 15):25.
4. Perse M, Cerar A. Dextran sodium sulphate colitis mouse model: traps and tricks. Journal of biomedicine & biotechnology. 2012; 2012:718617. [PubMed: 22665990]
5. Alex P, Zachos NC, Nguyen T, Gonzales L, Chen TE, Conklin LS, Centola M, Li X. Distinct cytokine patterns identified from multiplex profiles of murine DSS and TNBS-induced colitis. Inflammatory bowel diseases. 2009; 15:341–352. [PubMed: 18942757]
6. Egger B, Bajaj-Elliott M, MacDonald TT, Inglin R, Eysselein VE, Buchler MW. Characterisation of acute murine dextran sodium sulphate colitis: cytokine profile and dose dependency. Digestion. 2000; 62:240–248. [PubMed: 11070407]
7. Yan Y, Kolachala V, Dalmasso G, Nguyen H, Laroui H, Sitaraman SV, Merlin D. Temporal and spatial analysis of clinical and molecular parameters in dextran sodium sulfate induced colitis. PloS one. 2009; 4:e6073. [PubMed: 19562033]
8. Kabarowski JH. G2A and LPC: regulatory functions in immunity. Prostaglandins & other lipid mediators. 2009; 89:73–81. [PubMed: 19383550]
9. Yoder M, Zhuge Y, Yuan Y, Holian O, Kuo S, van Breemen R, Thomas LL, Lum H. Bioactive lysophosphatidylcholine 16:0 and 18:0 are elevated in lungs of asthmatic subjects. Allergy, asthma & immunology research. 2014; 6:61–65.
10. Zhuge Y, Yuan Y, van Breemen R, Degrand M, Holian O, Yoder M, Lum H. Stimulated bronchial epithelial cells release bioactive lysophosphatidylcholine 16:0, 18:0, and 18:1. Allergy, asthma & immunology research. 2014; 6:66–74.
11. Braun A, Treede I, Gotthardt D, Tietje A, Zahn A, Ruhwald R, Schoenfeld U, Welsch T, Kienle P, Erben G, Lehmann WD, Fuellekrug J, Stremmel W, Ehehalt R. Alterations of phospholipid concentration and species composition of the intestinal mucus barrier in ulcerative colitis: a clue to pathogenesis. Inflammatory bowel diseases. 2009; 15:1705–1720. [PubMed: 19504612]
12. Ehehalt R, Wagenblast J, Erben G, Lehmann WD, Hinz U, Merle U, Stremmel W. Phosphatidylcholine and lysophosphatidylcholine in intestinal mucus of ulcerative colitis patients. A quantitative approach by nanoElectrospray-tandem mass spectrometry. Scandinavian journal of gastroenterology. 2004; 39:737–742. [PubMed: 15513358]
13. Lauber K, Bohn E, Krober SM, Xiao YJ, Blumenthal SG, Lindemann RK, Marini P, Wiedig C, Zobywalski A, Baksh S, Xu Y, Autenrieth IB, Schulze-Osthoff K, Belka C, Stuhler G, Wesselborg S. Apoptotic cells induce migration of phagocytes via caspase-3-mediated release of a lipid attraction signal. Cell. 2003; 113:717–730. [PubMed: 12809603]
14. Peter C, Waibel M, Radu CG, Yang LV, Witte ON, Schulze-Osthoff K, Wesselborg S, Lauber K. Migration to apoptotic "find-me" signals is mediated via the phagocyte receptor G2A. The Journal of biological chemistry. 2008; 283:5296–5305. [PubMed: 18089568]
15. Radu CG, Yang LV, Riedinger M, Au M, Witte ON. T cell chemotaxis to lysophosphatidylcholine through the G2A receptor. Proceedings of the National Academy of Sciences of the United States of America. 2004; 101:245–250. [PubMed: 14681556]
16. Yan JJ, Jung JS, Lee JE, Lee J, Huh SO, Kim HS, Jung KC, Cho JY, Nam JS, Suh HW, Kim YH, Song DK. Therapeutic effects of lysophosphatidylcholine in experimental sepsis. Nature medicine. 2004; 10:161–167.
17. Nishioka H, Horiuchi H, Arai H, Kita T. Lysophosphatidylcholine generates superoxide anions through activation of phosphatidylinositol 3-kinase in human neutrophils. FEBS letters. 1998; 441:63–66. [PubMed: 9877166]

18. Nishi E, Kume N, Ueno Y, Ochi H, Moriwaki H, Kita T. Lysophosphatidylcholine enhances cytokine-induced interferon gamma expression in human T lymphocytes. Circulation research. 1998; 83:508–515. [PubMed: 9734473]
19. Cooper HS, Murthy SN, Shah RS, Sedergran DJ. Clinicopathologic study of dextran sulfate sodium experimental murine colitis. Laboratory investigation; a journal of technical methods and pathology. 1993; 69:238–249.
20. Kominsky DJ, Campbell EL, Ehrentraut SF, Wilson KE, Kelly CJ, Glover LE, Collins CB, Bayless AJ, Saeedi B, Dobrinskikh E, Bowers BE, MacManus CF, Muller W, Colgan SP, Bruder D. IFN-gamma-mediated induction of an apical IL-10 receptor on polarized intestinal epithelia. J Immunol. 2014; 192:1267–1276. [PubMed: 24367025]
21. Bligh EG, Dyer WJ. A rapid method of total lipid extraction and purification. Canadian journal of biochemistry and physiology. 1959; 37:911–917. [PubMed: 13671378]
22. Frasch SC, Berry KZ, Fernandez-Boyanapalli R, Jin HS, Leslie C, Henson PM, Murphy RC, Bratton DL. NADPH oxidase-dependent generation of lysophosphatidylserine enhances clearance of activated and dying neutrophils via G2A. The Journal of biological chemistry. 2008; 283:33736–33749. [PubMed: 18824544]
23. Frasch SC, Fernandez-Boyanapalli RF, Berry KA, Murphy RC, Leslie CC, Nick JA, Henson PM, Bratton DL. Neutrophils regulate tissue Neutrophilia in inflammation via the oxidant-modified lipid lysophosphatidylserine. The Journal of biological chemistry. 2013; 288:4583–4593. [PubMed: 23293064]
24. Bain CC, Mowat AM. The monocyte-macrophage axis in the intestine. Cellular immunology. 2014; 291:41–48. [PubMed: 24726741]
25. Platt AM, Bain CC, Bordon Y, Sester DP, Mowat AM. An independent subset of TLR expressing CCR2-dependent macrophages promotes colonic inflammation. J Immunol. 2010; 184:6843–6854. [PubMed: 20483766]
26. Bain CC, Scott CL, Uronen-Hansson H, Gudjonsson S, Jansson O, Grip O, Guilliams M, Malissen B, Agace WW, Mowat AM. Resident and pro-inflammatory macrophages in the colon represent alternative context-dependent fates of the same Ly6Chi monocyte precursors. Mucosal immunology. 2013; 6:498–510. [PubMed: 22990622]
27. Zigmond E, Varol C, Farache J, Elmaliah E, Satpathy AT, Friedlander G, Mack M, Shpigel N, Boneca IG, Murphy KM, Shakhar G, Halpern Z, Jung S. Ly6C hi monocytes in the inflamed colon give rise to proinflammatory effector cells and migratory antigen-presenting cells. Immunity. 2012; 37:1076–1090. [PubMed: 23219392]
28. Kiesler P, Fuss IJ, Strober W. Experimental Models of Inflammatory Bowel Diseases. Cellular and molecular gastroenterology and hepatology. 2015; 1:154–170. [PubMed: 26000334]
29. Waddell A, Ahrens R, Steinbrecher K, Donovan B, Rothenberg ME, Munitz A, Hogan SP. Colonic eosinophilic inflammation in experimental colitis is mediated by Ly6C(high) CCR2(+) inflammatory monocyte/macrophage-derived CCL11. J Immunol. 2011; 186:5993–6003. [PubMed: 21498668]
30. Moshkovits I, Reichman H, Karo-Atar D, Rozenberg P, Zigmond E, Haberman Y, Ben Baruch-Morgenstern N, Lampinen M, Carlson M, Itan M, Denson LA, Varol C, Munitz A. A key requirement for CD300f in innate immune responses of eosinophils in colitis. Mucosal immunology. 2016
31. Masterson JC, McNamee EN, Fillon SA, Hosford L, Harris R, Fernando SD, Jedlicka P, Iwamoto R, Jacobsen E, Protheroe C, Eltzschig HK, Colgan SP, Arita M, Lee JJ, Furuta GT. Eosinophil-mediated signalling attenuates inflammatory responses in experimental colitis. Gut. 2015; 64:1236–1247. [PubMed: 25209655]
32. Nava P, Koch S, Laukoetter MG, Lee WY, Kolegraff K, Capaldo CT, Beeman N, Addis C, Gerner-Smidt K, Neumaier I, Skerra A, Li L, Parkos CA, Nusrat A. Interferon-gamma regulates intestinal epithelial homeostasis through converging beta-catenin signaling pathways. Immunity. 2010; 32:392–402. [PubMed: 20303298]
33. Thelemann C, Eren RO, Coutaz M, Brasseit J, Bouzourene H, Rosa M, Duval A, Lavanchy C, Mack V, Mueller C, Reith W, Acha-Orbea H. Interferon-gamma induces expression of MHC class II on intestinal epithelial cells and protects mice from colitis. PloS one. 2014; 9:e86844. [PubMed: 24489792]

34. Jakubzick C, Gautier EL, Gibbings SL, Sojka DK, Schlitzer A, Johnson TE, Ivanov S, Duan Q, Bala S, Condon T, van Rooijen N, Grainger JR, Belkaid Y, Ma'ayan A, Riches DW, Yokoyama WM, Ginhoux F, Henson PM, Randolph GJ. Minimal differentiation of classical monocytes as they survey steady-state tissues and transport antigen to lymph nodes. Immunity. 2013; 39:599–610. [PubMed: 24012416]
35. Rivollier A, He J, Kole A, Valatas V, Kelsall BL. Inflammation switches the differentiation program of Ly6Chi monocytes from antiinflammatory macrophages to inflammatory dendritic cells in the colon. The Journal of experimental medicine. 2012; 209:139–155. [PubMed: 22231304]
36. Ito R, Shin-Ya M, Kishida T, Urano A, Takada R, Sakagami J, Imanishi J, Kita M, Ueda Y, Iwakura Y, Kataoka K, Okanoue T, Mazda O. Interferon-gamma is causatively involved in experimental inflammatory bowel disease in mice. Clinical and experimental immunology. 2006; 146:330–338. [PubMed: 17034586]
37. Sheikh SZ, Matsuoka K, Kobayashi T, Li F, Rubinas T, Plevy SE. Cutting edge: IFN-gamma is a negative regulator of IL-23 in murine macrophages and experimental colitis. J Immunol. 2010; 184:4069–4073. [PubMed: 20228197]
38. Cottone M, Orlando A, Renna S. Investigational agents for Crohn's disease. Expert opinion on investigational drugs. 2010; 19:1147–1159. [PubMed: 20836616]
39. Frasch SC, Zemski-Berry K, Murphy RC, Borregaard N, Henson PM, Bratton DL. Lysophospholipids of different classes mobilize neutrophil secretory vesicles and induce redundant signaling through G2A. J Immunol. 2007; 178:6540–6548. [PubMed: 17475884]
40. Bauer J, Liebisch G, Hofmann C, Huy C, Schmitz G, Obermeier F, Bock J. Lipid alterations in experimental murine colitis: role of ceramide and imipramine for matrix metalloproteinase-1 expression. PloS one. 2009; 4:e7197. [PubMed: 19787068]
41. Hogan SP, Waddell A, Fulkerson PC. Eosinophils in infection and intestinal immunity. Current opinion in gastroenterology. 2013; 29:7–14. [PubMed: 23132211]
42. Woodruff SA, Masterson JC, Fillon S, Robinson ZD, Furuta GT. Role of eosinophils in inflammatory bowel and gastrointestinal diseases. Journal of pediatric gastroenterology and nutrition. 2011; 52:650–661. [PubMed: 21593640]
43. Askenase MH, Han SJ, Byrd AL, Morais da Fonseca D, Bouladoux N, Wilhelm C, Konkel JE, Hand TW, Lacerda-Queiroz N, Su XZ, Trinchieri G, Grainger JR, Belkaid Y. Bone-Marrow-Resident NK Cells Prime Monocytes for Regulatory Function during Infection. Immunity. 2015; 42:1130–1142. [PubMed: 26070484]
44. Shouval DS, Biswas A, Goettel JA, McCann K, Conaway E, Redhu NS, Mascanfroni ID, Al Adham Z, Lavoie S, Ibourk M, Nguyen DD, Samsom JN, Escher JC, Somech R, Weiss B, Beier R, Conklin LS, Ebens CL, Santos FG, Ferreira AR, Sherlock M, Bhan AK, Muller W, Mora JR, Quintana FJ, Klein C, Muise AM, Horwitz BH, Snapper SB. Interleukin-10 receptor signaling in innate immune cells regulates mucosal immune tolerance and anti-inflammatory macrophage function. Immunity. 2014; 40:706–719. [PubMed: 24792912]
45. Shouval DS, Ouahed J, Biswas A, Goettel JA, Horwitz BH, Klein C, Muise AM, Snapper SB. Interleukin 10 receptor signaling: master regulator of intestinal mucosal homeostasis in mice and humans. Advances in immunology. 2014; 122:177–210. [PubMed: 24507158]
46. Zigmond E, Bernshtein B, Friedlander G, Walker CR, Yona S, Kim KW, Brenner O, Krauthgamer R, Varol C, Muller W, Jung S. Macrophage-restricted interleukin-10 receptor deficiency, but not IL-10 deficiency, causes severe spontaneous colitis. Immunity. 2014; 40:720–733. [PubMed: 24792913]
47. Stillie R, Stadnyk AW. Role of TNF receptors, TNFR1 and TNFR2, in dextran sodium sulfate-induced colitis. Inflammatory bowel diseases. 2009; 15:1515–1525. [PubMed: 19479745]
48. Wang K, Han G, Dou Y, Wang Y, Liu G, Wang R, Xiao H, Li X, Hou C, Shen B, Guo R, Li Y, Shi Y, Chen G. Opposite role of tumor necrosis factor receptors in dextran sulfate sodium-induced colitis in mice. PloS one. 2012; 7:e52924. [PubMed: 23285227]
49. Bradley JR. TNF-mediated inflammatory disease. The Journal of pathology. 2008; 214:149–160. [PubMed: 18161752]

50. Peyrin-Biroulet L. Anti-TNF therapy in inflammatory bowel diseases: a huge review. Minerva gastroenterologica e dietologica. 2010; 56:233–243. [PubMed: 20485259]

51. Sandborn WJ, Hanauer S, Loftus EV Jr, Tremaine WJ, Kane S, Cohen R, Hanson K, Johnson T, Schmitt D, Jeche R. An open-label study of the human anti-TNF monoclonal antibody adalimumab in subjects with prior loss of response or intolerance to infliximab for Crohn's disease. The American journal of gastroenterology. 2004; 99:1984–1989. [PubMed: 15447761]

52. Muzaki AR, Tetlak P, Sheng J, Loh SC, Setiagani YA, Poidinger M, Zolezzi F, Karjalainen K, Ruedl C. Intestinal CD103(+)CD11b(−) dendritic cells restrain colitis via IFN-gamma-induced anti-inflammatory response in epithelial cells. Mucosal immunology. 2016; 9:336–351. [PubMed: 26174764]

53. Gurtner GJ, Newberry RD, Schloemann SR, McDonald KG, Stenson WF. Inhibition of indoleamine 2,3-dioxygenase augments trinitrobenzene sulfonic acid colitis in mice. Gastroenterology. 2003; 125:1762–1773. [PubMed: 14724829]

54. Kominsky DJ, Keely S, MacManus CF, Glover LE, Scully M, Collins CB, Bowers BE, Campbell EL, Colgan SP. An endogenously anti-inflammatory role for methylation in mucosal inflammation identified through metabolite profiling. J Immunol. 2011; 186:6505–6514. [PubMed: 21515785]

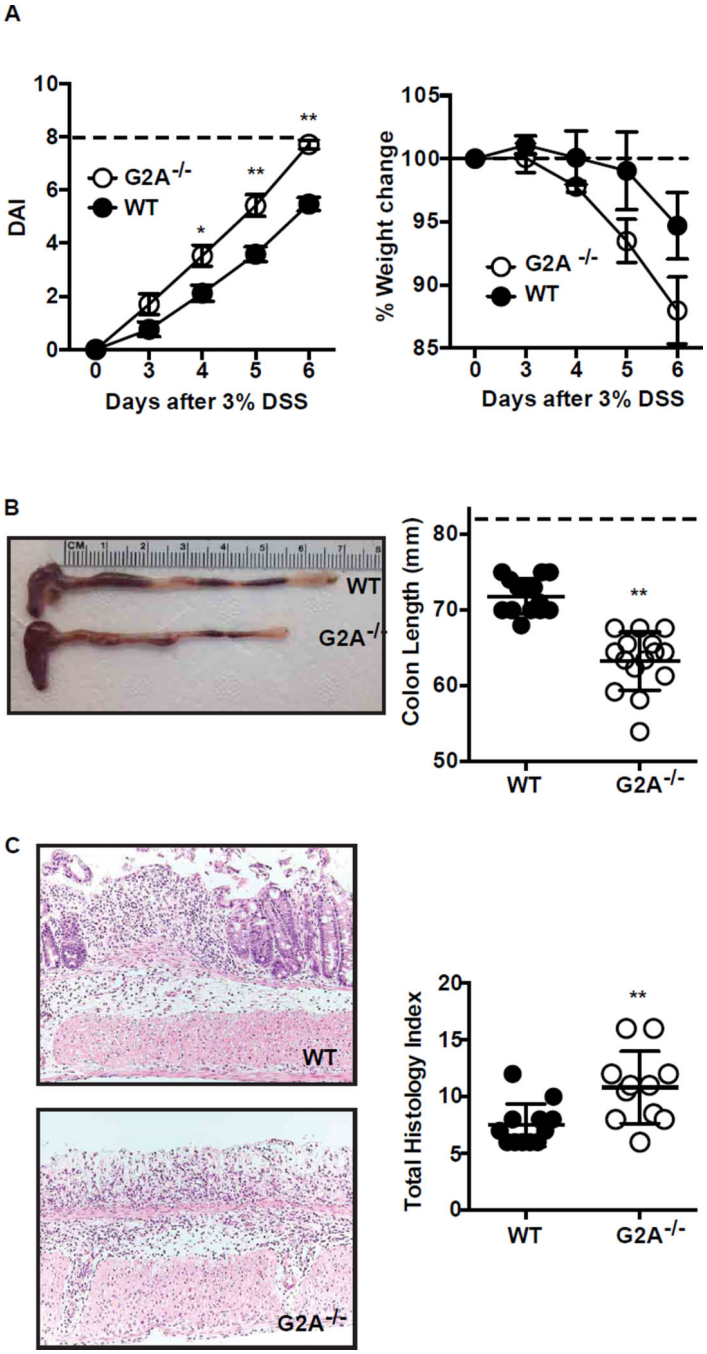

Figure 1. Loss of G2A receptor signaling exacerbates DSS-induced colitis

A, disease activity (DAI) *(left)* and % change in weight *(right)* were determined daily during DSS administration as described in Experimental Procedures. Dotted line indicates maximum DAI score (left) or initial body weight at day 0 (right). *B*, colon length as a measure of disease severity was determined on day 6 after 3% DSS administration. *Left*, representative photograph of WT and G2A$^{-/-}$ colons. *Right*, summated colon lengths for each genotype. Dotted line represents colon length of water control animals (See Supplemental Fig. 1B). *C, Left*, representative histologic images of the distal colon on day 6.

Right, quantitative total histologic index. Data represent mean ± SEM; n=15, *p<0.05 versus WT; ** p<0.01 versus WT.

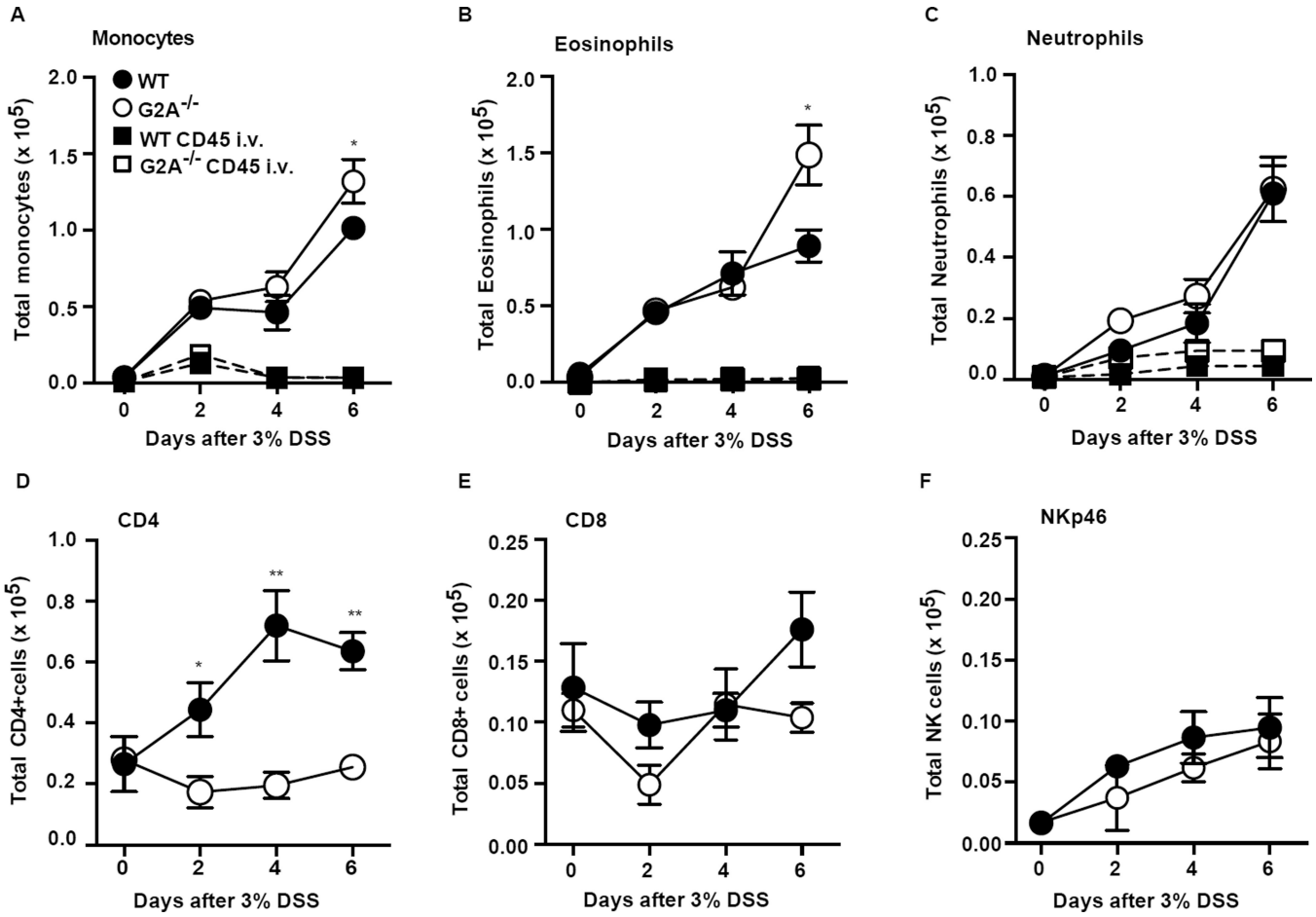

Figure 2. G2A$^{-/-}$ mice show altered recruitment of immune cells over the course of DSS-induced colitis

A–F, immune cell types were determined by flow cytometry following digestion as described in Experimental Procedures. Gating strategy is described in Experimental Procedures and Supp. Fig. 1E. Note differences in scale. *Square symbols* denote myeloid cells tagged with *i.v.* anti-CD45 (See Experimental Procedures). Data represent mean ± SEM; n=8–10, *p<0.05 compared to WT; **< 0.01 compared to WT.

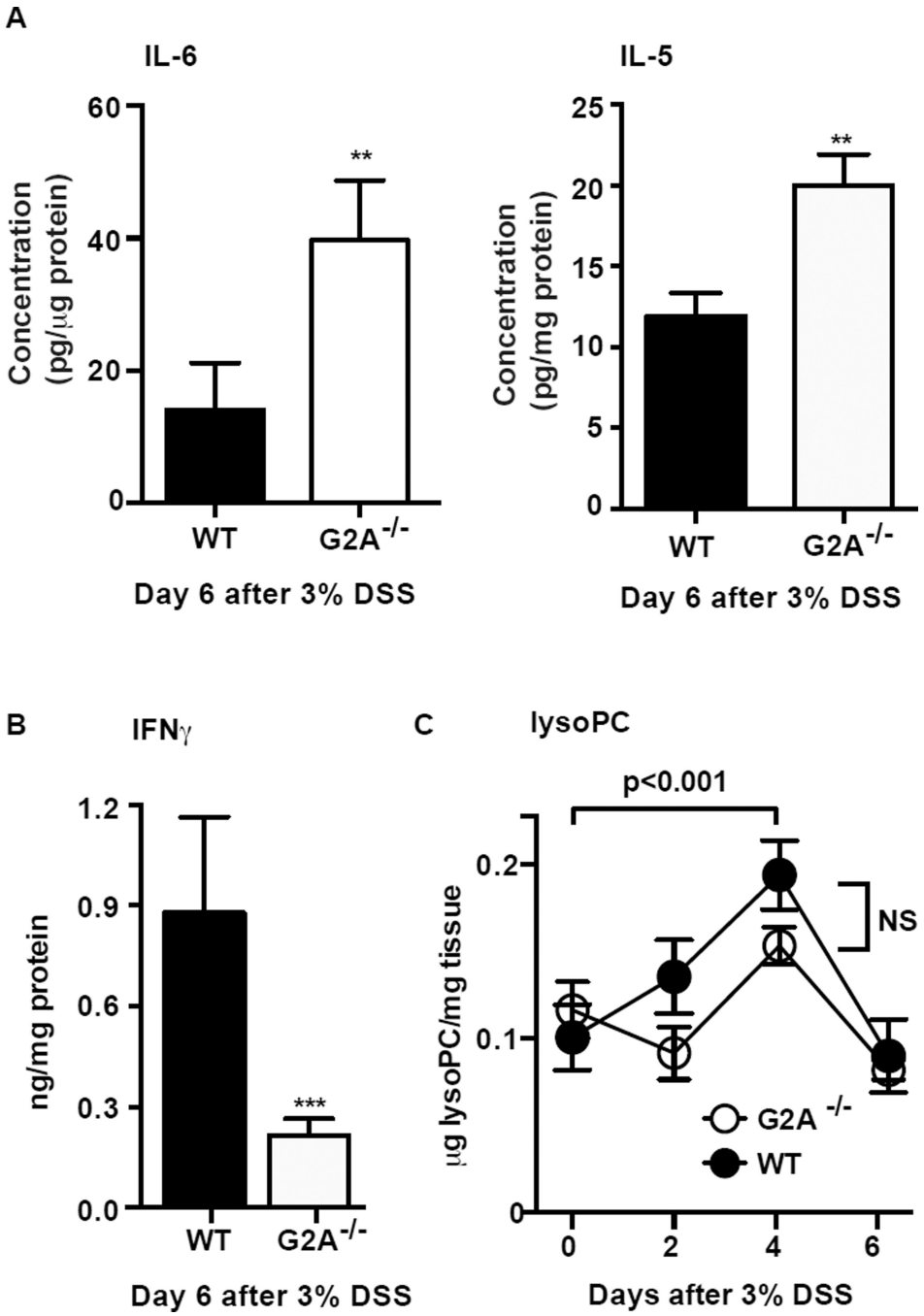

Figure 3. Loss of G2A receptor signaling results in altered cytokine production

IL-6, IL-5 (*A*) and IFNγ (*B*) were among cytokines measured in homogenates from a 1 cm section of the distal colon by MesoScale Discovery Platform 6 days after administration of 3% DSS. Data represents mean ± SEM; n=10, ** p< 0.01 versus WT; *** p< 0.001 versus WT. *C*, lysophosphatidylcholine (lysoPC) was quantified by LC-MS/MS in whole colon tissue over a time course of DSS colitis and showed a significant increase 4 days after administration of DSS. No difference was detected between the genotypes. Data represent mean ± SEM; n=6.

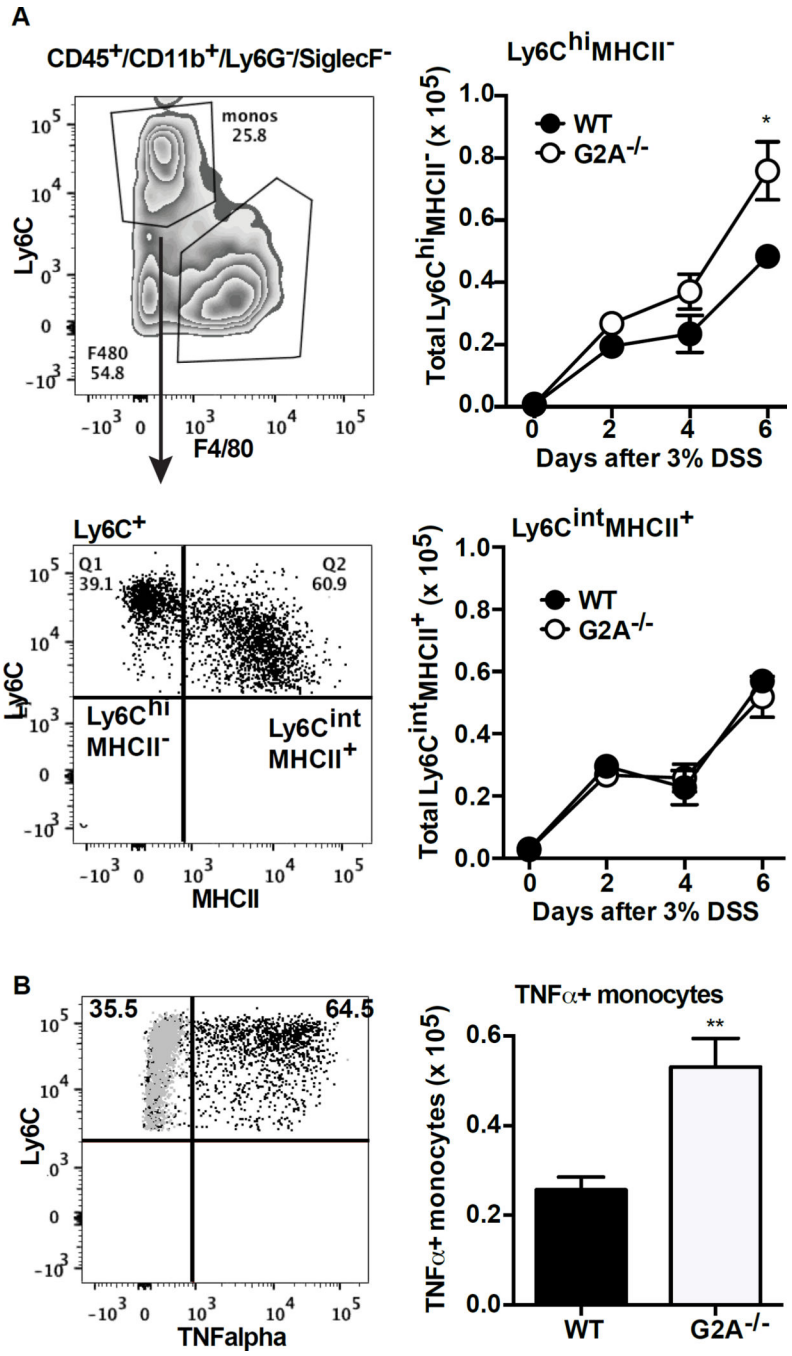

Figure 4. G2A$^{-/-}$ mice have more TNFα^{+} pro-inflammatory monocytes during DSS-induced colitis than WT

A, representative flow cytometry plot demonstrating gating strategy to separate Ly6C^{hi}MHCII^{-} from Ly6C^{int}MHCII^{+} monocytes (*left*). Total Ly6C^{hi}MHCII^{-} and Ly6C^{int}MHCII^{+} monocytes were determined by multiplying the percentage by the total number of monocytes from Fig. 2 (*right).* Data represents mean ± SEM; n=10, *p<0.05 compared to WT. *B*, representative flow plot demonstrating intracellular TNFα staining in the Ly6C positive monocytes (*left*). Gray dots are isotype antibody controls. Total numbers of TNFα^{+} monocytes *(right)* was determined by multiplying the percentage of TNFα^{+} cells

by the total number of monocytes from Fig.2. Data represents mean ±SEM; n=10, ** $p<0.01$ compared to WT.

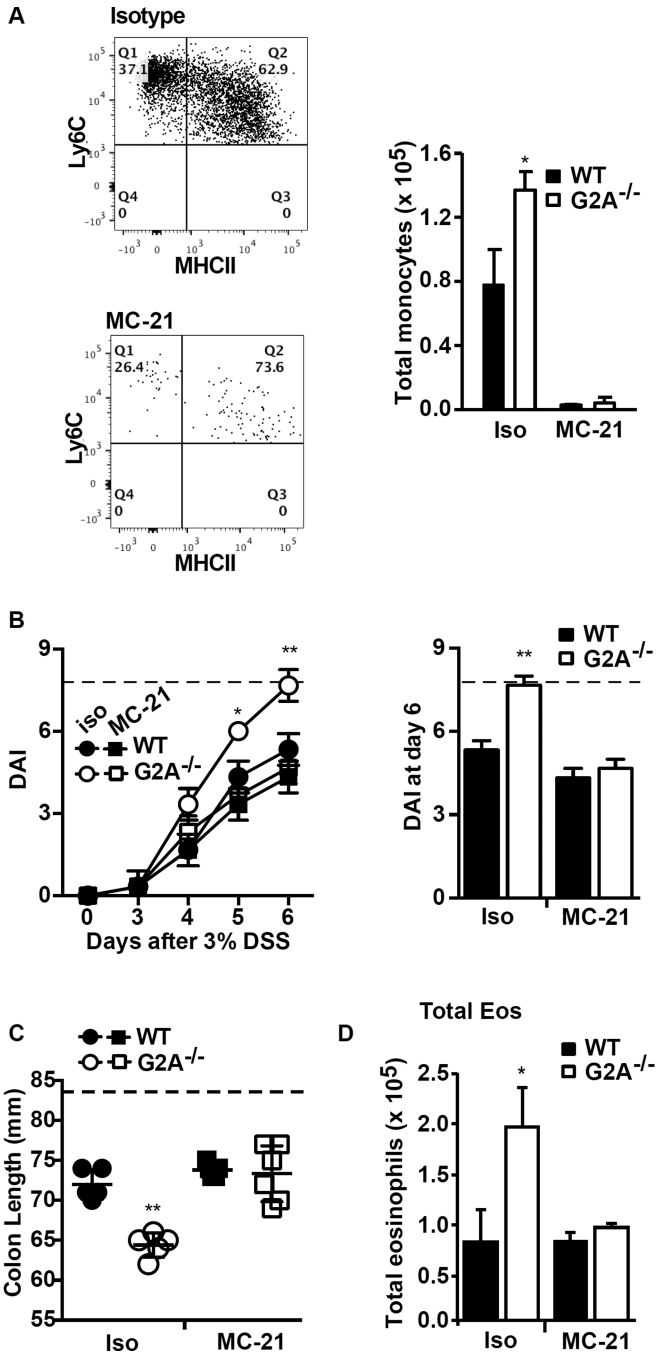

Figure 5. Depletion of monocytes limits disease severity in G2A$^{-/-}$ mice and reduces eosinophil numbers

Mice were treated with anti-CCR2 clone MC-21 (MC-21) or isotype antibody as described in Experimental Procedures. *A*, monocytes were depleted with MC-21: *Left*, representative flow plot demonstrating efficient depletion of monocytes. *Right*, total monocytes were significantly reduced in MC-21 treated animals (versus isotype treated) for both genotypes. *B*, Disease activity index (DAI) was determined in MC-21 or isotype treated mice over the timecourse of DSS exposure (*left*) and in an expanded representation for day 6 of DSS exposure (*right*). Dotted line indicates maximum DAI score. *C*, colon length was determined

at day 6 following administration of DSS in MC-21 and isotype treated animals. Dotted line represents colon length of water control animals. *D*, total numbers of eosinophils were determined with and without monocyte depletion with MC-21. Data represent mean ± SEM n=10, *p<0.05 and **p<0.01 compared to WT isotype, WT MC-21 and G2A$^{-/-}$ MC-21.

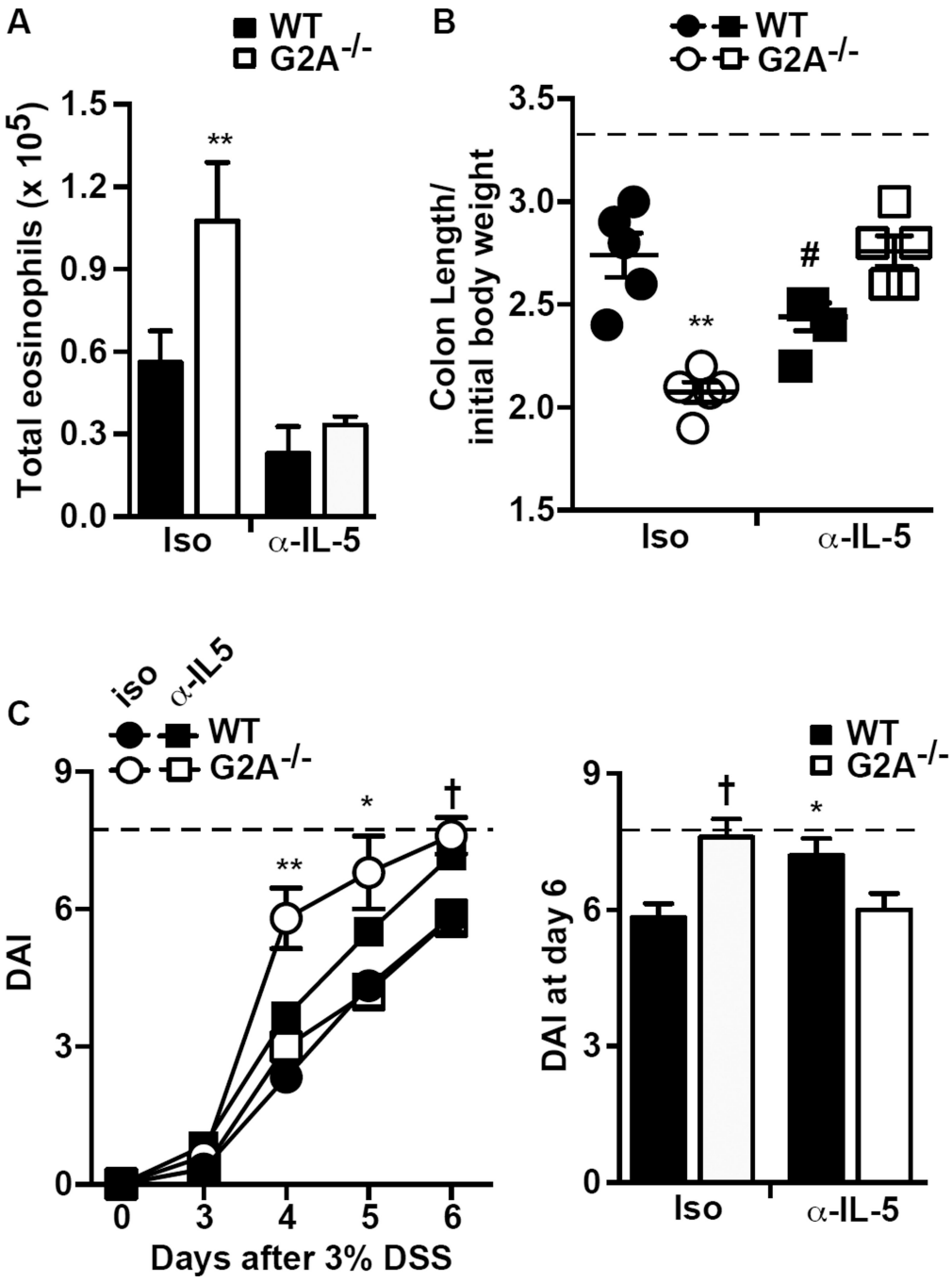

Figure 6. Treatment with α-IL-5 reduces eosinophil numbers and disease severity in G2A$^{-/-}$ mice

Mice were treated with α-IL-5 clone TRFK5 or isotype control antibody as described in Experimental Procedures. *A*, Total eosinophils at day 6 were determined as described in Fig. 2. *B*, colon length normalized to initial body weight and *C*, disease activity (DAI) determined over the timecourse of DSS exposure (*left*) and in an expanded representation for day 6 after DSS exposure (*right*). Dotted line represents colon length per initial body weight from water control animals (B) or maximum DAI score (C). Data represents mean ± SEM; n=10, **p<0.01 compared to WT isotype, WT α-IL-5 and G2A$^{-/-}$ α-IL-5; *p<0.05

compared to G2A$^{-/-}$ α-IL-5 or WT isotype; $^{\#}p<0.05$ compared to WT isotype, G2A$^{-/-}$ isotype and G2A$^{-/-}$ α-IL-5; $^{\dagger}p<0.01$ compared to WT isotype or G2A$^{-/-}$ α-IL-5.

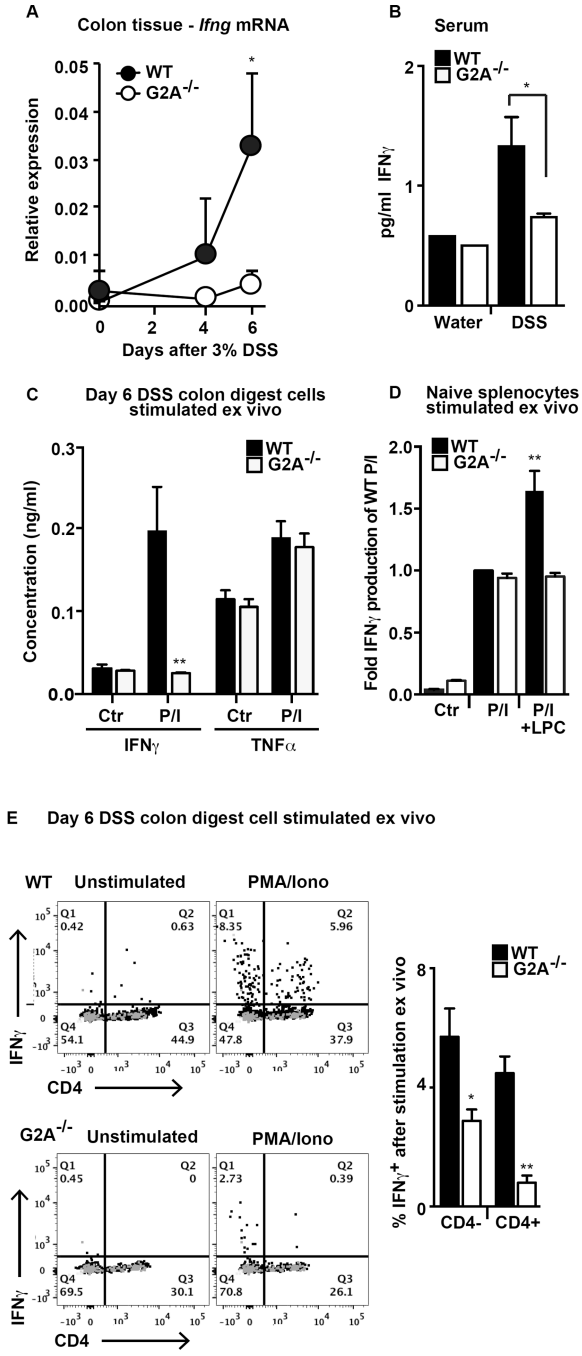

Figure 7. IFNγ production is deficient in colon tissues and stimulated colonic lymphocytes from G2A$^{-/-}$ mice

A, Ifnγ gene expression was determined by qPCR from sections of distal colon over the timecourse of DSS-induced colitis. Data represents mean ± SEM; n=10, *p<0.05 compared to G2A$^{-/-}$. *B*, serum was collected from whole blood from naïve mice or at day 6 after administration of DSS and IFNγ concentration was determined as described in Fig. 3. Data represent mean ± SEM; n=6–8, *p<0.05. *C*, IFNγ and TNFα were measured by ELISA in cell-free supernatants following stimulation of cells from digested colons with PMA and ionomycin (P/I) for 4 hours. Data represent mean ± SEM; n=10, **p<0.01 compared to

stimulated WT. *D*, IFNγ was measured in cell-free supernatants following stimulation of splenocytes from naive animals as described in *C* in the presence or absence of 10μM lysoPC (LPC). Data are displayed as fold of stimulated WT and represent mean ± SEM; n=4–6, **p<0.01 compared to stimulated WT, stimulated G2A$^{-/-}$ and stimulated G2A$^{-/-}$ +LPC *E*, intracellular IFNγ staining in control and stimulated (PMA and ionomycin for 4 hours) colon digest cells from day 6 DSS in the presence of brefeldin A. Representative flow plots demonstrating intracellular IFNγ staining in control or stimulated B220^{-}SSC^{lo} CD4^{+} and CD4^{-} lymphocytes *(left)*. Gray dots are stained with isotype control antibody. The percent of stimulated B220^{-}CD4^{-} or B220^{-}CD4^{+} lymphocytes staining positive for IFNγ in WT or G2A$^{-/-}$ mice is shown *(right)*. Data represent mean ± SEM; n=10, *p<0.05 compared to WT; **p<0.01 compared to WT.

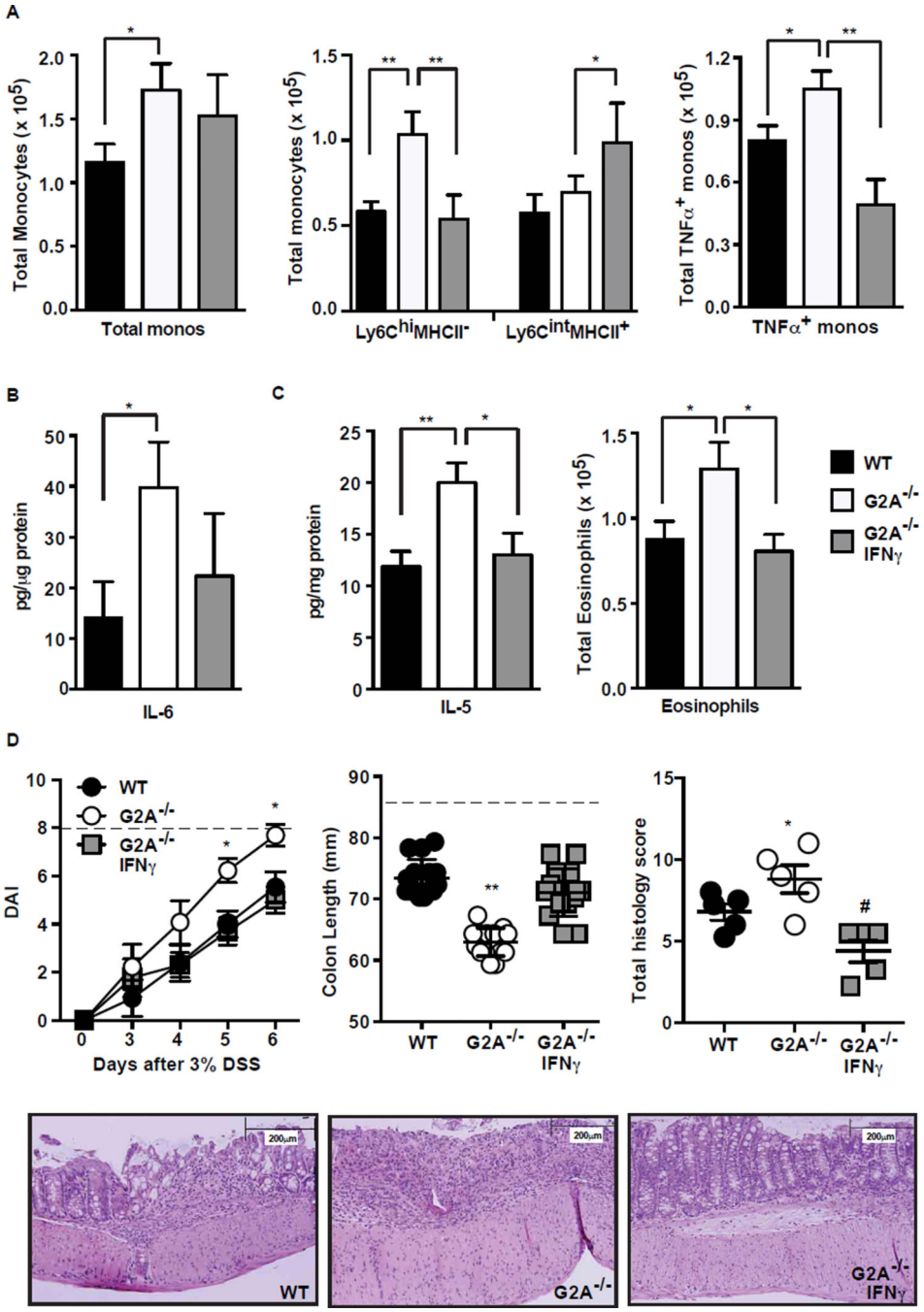

Figure 8. Provision of IFNγ to G2A$^{-/-}$ mice enhances anti-inflammatory monocyte programming, reduces IL-5 and eosinophils and limits disease severity

G2A$^{-/-}$ mice were treated with 5 μg IFNγ on days 3 and 5 after administration of 3% DSS and harvested at day 6. *A*, total monocytes, Ly6C^{hi}MHCII^{-} monocytes and Ly6C^{int}MHCII^{+} monocytes and TNFα^{+} monocytes were determined as described in Fig. 2 and 4. Data represent mean ± SEM; n=15, *p<0.05, **p<0.01. *B*, IL-6 concentration in a distal section of colon tissue was determined as described in Fig. 3. Data represent mean ± SEM; n=6, *p<0.05. *C*, IL-5 concentration was determined as described in *B* and total eosinophil numbers were determined as described in Fig. 2. Data represent mean ± SEM; n=15,

*p<0.05; **p<0.01. *D*, disease activity (DAI) *(left)*, colon length *(middle)* and total histologic index *(right)* were determined as described in Fig.1. Dotted line represents maximum DAI score (*left*) or colon length of water control animals (*middle*). *Lower*, representative histologic images of WT, $G2A^{-/-}$ or IFNγ treated $G2A^{-/-}$ mice. Data represent mean ± SEM; n=15, *p<0.05 compared to WT; **p<0.01 compared to WT and $G2A^{-/-}$ IFNγ; $^{\#}$p<0.01 compared to $G2A^{-/-}$.